PROCEEDINGS OF SPIE

SPIEDigitalLibrary.org/conference-proceedings-of-spie

Spectral reflectance measurements of snow and snow covered objects: experimental studies compared with mathematical models

Selj, Gorm , Mikkelsen, Alexander

Gorm K. Selj, Alexander Mikkelsen, "Spectral reflectance measurements of snow and snow covered objects: experimental studies compared with mathematical models," Proc. SPIE 11865, Target and Background Signatures VII, 1186504 (12 September 2021); doi: 10.1117/12.2597953

SPIE.

Event: SPIE Security + Defence, 2021, Online Only

Downloaded From: https://www.spiedigitallibrary.org/conference-proceedings-of-spie on 18 Oct 2021 Terms of Use: https://www.spiedigitallibrary.org/terms-of-use

Spectral reflectance measurements of snow and snow covered objects – experimental studies compared with mathematical models

Gorm K. Selj,[a, *] Alexander Mikkelsen[a]
[a]Norwegian Defence Research Establishment, Instituttveien 20, Kjeller, Norway, 2007

ABSTRACT

In this study, we have investigated reflectance spectra of different snow types under various conditions. Snow reflectance is interesting from a camouflage point of view as snow covers large land areas in many parts of the world during winter, at high altitudes or high (or low) latitudes. Snow reflectance of incident light differs from light reflected by other natural constituents such as soil and vegetation by the high reflectance, particularly in the visible wavelength range. It is therefore important to characterize various snow reflectance properties further. From a concealment point of view, it is also important to study differences – and similarities – in reflectance of snow and vegetation (including frost-covered vegetation) beyond the wavelengths visible to the naked eye. Especially because reflected light from vegetation is dominated more by water content as the wavelength increases. Finally, it is of interest to study the effects on snow coverage needed to mask signatures of underlying objects and to observe if snow reflectance, as a function of thin layers fits well to existing models of light reflected by thin, semi-transparent layers. We found that fresh powder snow, wet snow, coarse snow, and deep (and older) snow layers had similar reflectance spectra, albeit with important differences. Fresh powder snow reflected more light than wet, older or coarse snow that had lower reflectance values, yet distinctly different from vegetation for wavelengths below about 1000 nm. For longer wavelengths, however, the differences between pure snow and green vegetation were much less pronounced. Finally, the reflectance of frost-covered vegetation deviated from pure vegetation, but to a much less degree than pure snow. Layer thickness needed to mask underlying surfaces was studied for coarse snow distributed evenly onto a green reference object, and we found the characteristic thickness (corresponding to specific weights of snow per area) needed to effectively hide the spectral reflectance signatures.

Keywords: Spectral imaging, reflectance, mathematical models, snow, vegetation, remote sensing, solar energy harvesting, camouflage materials, transmittance, extinction coefficients.

***Gorm Krogh Selj**, E-mail: gorm-krogh.selj@ffi.no

1 INTRODUCTION

Snow reflectance is interesting from a camouflage point of view as snow covers large land areas in many parts of the world during winter, at high altitudes or high (or low) latitudes. Snow reflectance of incident light differs from light reflected by other natural constituents such as soil, vegetation, and ice by the high reflectance, particularly in the visible wavelength range[1,2]. Therefore, it is important to characterize various snow reflectance properties further. In addition, from a concealment point of view, it is important to study differences – and similarities – in reflectivity of relevant terrain signatures such as snow and vegetation[3]. That includes frost-covered vegetation beyond the wavelengths visible to the naked eye, as it is known that reflected light from vegetation is dominated more by water content as the wavelength increases.

In the coming years, electro-optical sensors are expected to become more capable, proliferated, cheap, and small. In addition, analysis of data become more sophisticated, tailored, and accessible, and remote sensing applications are expected to be more important. The task of concealing an object is therefore becoming increasingly challenging and will require camouflage materials (or camouflage strategies) that adapts the spectral properties, reflectance as well as transmittance, of the backgrounds of operation[4-9].

In particular, the interaction of solar radiation with snow covered areas are interesting to study further to develop effective winter camouflage strategies, as well as precise interpretations of signatures captured for land mapping-based remote sensing purposes[10,11]. Snow, which is basically a granular mix of ice and air[1,11], is known to be a granular material with

Target and Background Signatures VII, edited by Karin U. Stein, Ric Schleijpen, Proc. of SPIE
Vol. 11865, 1186504 · © 2021 SPIE · CCC code: 0277-786X/21/$21 · doi: 10.1117/12.2597953

Downloaded From: https://www.spiedigitallibrary.org/conference-proceedings-of-spie on 18 Oct 2021
Terms of Use: https://www.spiedigitallibrary.org/terms-of-use

complex microstructure[1,2]. As snow is not optically opaque, but rather semi-transparent, the distribution of incoming solar light that is transmitted through snow will also affect the signatures any electro-optical sensor will capture given by the light that eventually is being scattered back towards it. Although studies on snow transmittance have been done earlier[2], little is known about how variations in snow layer thickness, wavelength-dependencies, and snow type will influence on the measured reflectance when covering an underlying object. In addition, the current knowledge on snow transmittance data above approximately 900 nm seem to be lacking, very scarce,[2] and rely on snow transmittance measurements that are complex in nature.

In addition, it has been shown that there are similarities between granular materials, such as snow and soil, when studying length scales much larger than the wavelength[11,12]. More knowledge on the optical characteristics of snow may therefore be of relevance in applications where there is no snow on the ground.

In this paper, we present two main results. Firstly, we present observations of experimentally obtained reflectance spectra (350 – 2500 nm) of various types of snow and green vegetation, and of snow layer thicknesses on measured reflectance. We found that fresh powder snow, wet snow, coarse snow and deep (and older) snow layers had similar shaped reflectance spectra, still with characteristic differences. Fresh powder snow reflected more light than wet, older or coarse snow that achieved lower reflectance values, yet distinctly different from vegetation for wavelengths below about 1000 nm. For longer wavelengths, however, the differences between pure snow and green vegetation were much smaller.

Snow layer thicknesses needed to mask underlying surfaces were studied for wet and coarse snow distributed evenly onto a reference textile. We were then able to find the characteristic snow thicknesses, defined in this paper as reflectance threshold values, needed to effectively hide characteristic spectral reflectance signatures, given by the underlying, artificial object. We found that light penetrated deeper into the snow pack layer in the visible wavelength range and shallower with increased wavelengths, which is opposite from green vegetation spectra[13,14], but in accordance with similar measurements on snow[15].

Secondly, we investigated the applicability of a mathematical model used in a predicative sense, providing answers to problems that can be difficult to solve by direct measurements of inherent (snow) optical properties. Snow extinction coefficients, a material parameter describing how effective the snow pack hinders light transmittance[2] were calculated for selected wavelengths (700, 1100, 1300, and 1700 nm) by using a mathematical model for thin, optically semi-transparent structures[16] in combination with experimental reflectance data. Hence, our new approach allow for snow transmittance properties estimations through modelling and simple reflectance measurements, and not transmittance measurements, considered to be more difficult and complex[2].

We expect the results found in this study to be valuable to any further improvements and developments in advanced (semi-transparent and multi-layered) camouflage products. The results are also expected to be of interest for remote sensing purposes where snow covered land areas are mapped continuously by optical sensors[10,11,15,17-26] as well as for effective all-year solar energy harvesting[27-30] and in understanding plant photosynthesis onset during early spring[31].

2 EXPERIMENTAL SETUP AND METHOD

2.1 Spectral reflectance measurements

A HR 1024 spectrophotometer (Spectra Vista Corporation) was used to measure the diffuse reflectance of all snow and vegetation samples (Fig. 1) for incoming light of wavelengths between 350 and 2500 nm. All measurements were carried out outdoor under stable illumination conditions (sunny and clear sky), with little or no wind, and with a measurement area of about 8 x 5 cm. A Lambertian white reference plate was used between each measurement series to calibrate the instrument.

The snow types studied in this paper were dry powder snow, compact (and coarse) snow from deeper layers, coarse surface snow and wet snow, all being measured in Norway. The snow type chosen for snow layer measurements, aiming to estimate the snow extinction coefficient for different wavelengths, was wet and coarse snow measured under melting temperatures during springtime in southeast Norway. The spectral reflectance measurements of vegetation (green spruce needles and fur pine needles) were captured in Norway (October) and in Storkow, Germany, during wintertime (Feb. 2018), respectively. Figure 1 shows the measurement set-up used and sample preparations.

Downloaded From: https://www.spiedigitallibrary.org/conference-proceedings-of-spie on 18 Oct 2021
Terms of Use: https://www.spiedigitallibrary.org/terms-of-use

Because it was difficult to exactly measure the thicknesses of the snow layers for the thinnest snow layers, the effective thicknesses were obtained indirectly by controlled weight and area measurements. The snow layer thickness is an important input value in a theoretical extinction model (see Ch. 3) for estimating the snow extinction coefficient. We obtained the effective snow layer thickness by constraining the snowpack area (with a plastic rack and with minimum compression of the snowpack, see Fig. 1) and then measured the corresponding weight of the snowpack after each reflectance measurement. Table 1 lists data on the snow layers used for the measurements.

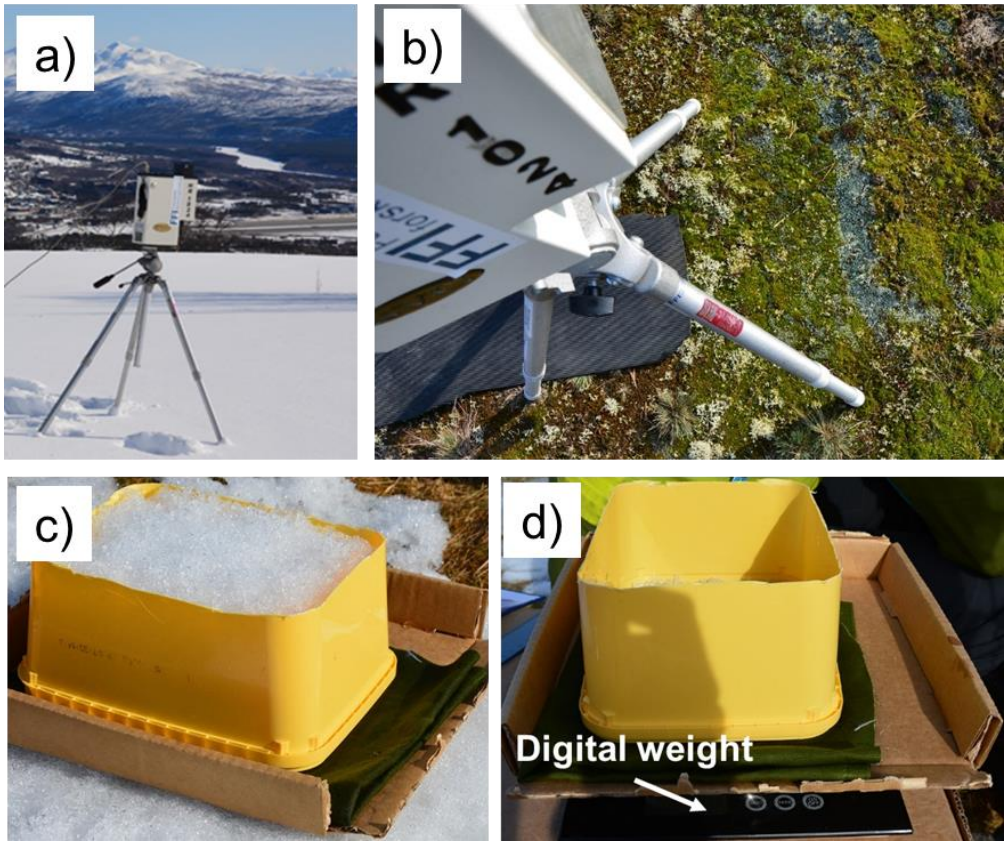

Figure 1. Experimental setup: Field spectrophotometer used for (a) snow and (b) vegetation reflectance measurements. (c) Control of snowpack thickness and size. (d) Measurement of snow weight for effective weight per area calculations.

2.2 Snow layer thickness data – estimation of effective thickness

Table 1 shows snow parameters measured for estimation of the thicknesses of the unique snow layers used in the reflectance measurements, and for calculations of snow extinction coefficients.

Table 1. Snow parameters for snow layer thickness estimations.

Snow weight (g)	66	174	235	359	750	961
Area (cm^2)	208	208	208	208	208	208
Measured thickness (cm)					6.30	8.35
Mass per area (mg/cm^2)	317	837	1130	1726	3606	4620
Mass density (g/cm^3)					0.57	0.55
Estimated snow layer thickness (cm)	0.57	1.49	2.02	3.08	6.30	8.35

Downloaded From: https://www.spiedigitallibrary.org/conference-proceedings-of-spie on 18 Oct 2021
Terms of Use: https://www.spiedigitallibrary.org/terms-of-use

3 THEORETICAL CONSIDERATIONS ON REFLECTANCE IN SEMI-TRANSPARENT MATERIAL

The experimental results presented in this paper have been fitted to and compared with a mathematical model for thin, semi-transparent structures, hereby referred to as the extinction model[16]. The model is simple to use, but has also been found to be valuable in explaining several optical features of material samples such as thin, semi-transparent biomaterial and synthetic materials[13,14]. As the model may not be well known to the reader, we present the basic content briefly below, and refer to the literature for further details [16,32].

3.1 The extinction model

The extinction model was derived by Wilhelm[16] and originally used to describe quantitatively the reflectance, transmittance, and absorptance by textiles in terms of specific reflection and absorption characteristics of fibers. The model builds on the Stokes equations for transmittance t_n and reflectance r_n of n plates:

$$t_n = \frac{c-c^{-1}}{cd^n-c^{-1}d^{-n}}, \tag{1}$$

$$r_n = \frac{d-d^{-n}}{cd^n-c^{-1}d^{-n}}, \tag{2}$$

where *c* and *d* are constants that only depend on the transmittance and reflectance of the single plates. The equations above were fitted to textile materials of different thicknesses expressed as weight per area by defining $c = 1/\alpha$ and $d = e^k$. Here the constant α is the reflectivity of the material when the thickness is taken to the extreme limit, *k* the extinction coefficient, while the constant e^{-kw} is the energy lost by absorption in a unit weight per area of material. Substituting *n* with *w*, which is the weight per unit area, and using the new definitions results in the following[16]:

$$t_w = \frac{(1-\alpha^2)e^{-kw}}{1-\alpha^2e^{-2kw}}, \tag{3}$$

$$r_w = \frac{\alpha(1-e^{-2kw})}{1-\alpha^2e^{-2kw}}. \tag{4}$$

The corresponding absorptance is given by: a_w = 1 - r_w - t_w.

For semi-transparent samples (such as snow, vegetation and thin artificial material) we have to account for the optical characteristics of both the i) sample and the ii) underlying background[13,14]. The spectral characteristics of the background should be included for correct modelling. If the reflectance of the background is given by β, expressions for the reflected, transmitted, and absorbed light of the system (sample and background) can be expressed as[16]:

$$\left(\frac{I_r}{I_0}\right)_{\text{syst.}} = r_w + t_w^2\beta + t_w^2r_w\beta^2 + t_w^2r_w^2\beta^3 + \cdots = r_w + \frac{t_w^2\beta}{1-r_w\beta}, \tag{5}$$

$$\left(\frac{I_t}{I_0}\right)_{\text{syst.}} = t_w(1-\beta) + t_wr_w\beta(1-\beta) + t_wr_w^2\beta^2(1-\beta) + t_wr_w^3\beta^3(1-\beta) \ldots = \frac{t_w(1-\beta)}{1-r_w\beta}, \tag{6}$$

$$\left(\frac{I_a}{I_0}\right)_{\text{syst.}} = 1 - \left(\frac{I_r}{I_0}\right)_{\text{syst.}} - \left(\frac{I_t}{I_0}\right)_{\text{syst.}} = \frac{a_w(1+\beta)(t_w-r_w)}{1-r_w\beta}. \tag{7}$$

3.2 Snow scattering assumptions

A simplified assumption on the scattering of light in snow can be justified to hold in the visible and near-infrared wavelengths[2]. Light is scattered by the snow grains, which typically exceed the wavelength in size, which means that the scattering is in the regime of geometrical optics. In addition, the index of refraction is reported not to vary much with wavelength[1,2] in this range, which means that reflectivity values (reflection values obtained at infinite snow layer thicknesses) are thought to be near-constant with wavelength. Furthermore, when applying the mathematical extinction model to our experimental reflectance data, we have assumed snow as a high number of thin layers of snow material in a stack consisting of a high number of correspondingly thin layers, and where each of the snow layers are assumed to be partially transparent to incident light.

Downloaded From: https://www.spiedigitallibrary.org/conference-proceedings-of-spie on 18 Oct 2021
Terms of Use: https://www.spiedigitallibrary.org/terms-of-use

4 RESULTS PART ONE – SPECTRAL REFLECTANCE OF SNOW

In this section, we present experimental results from the spectral reflectance measurements on different snow types, vegetation. In addition, snow reflectance is shown as a function of solar angle.

4.1 Snow – dry powder, coarse and wet

Figure 2 shows the spectral reflectance of dry, powder snow in the wavelength range 350 nm to 2500 nm (measured outdoor by a spectrophotometer under stable illumination conditions). Each graph corresponds to an average of 5-10 measurements carried out at the same (snow) spot at temperatures below the freezing point of water. We observed that all the dry (powder) snow areas measured resulted in similar reflectance spectra, with reflectance values decreasing gradually with increasing wavelength, starting from close to 100 % at 400 nm, down to a few percent reflected light at 1500 nm. Above 1450 nm, two reflectance peaks were seen (at about 1850 and 2250 nm) for the dry snow reflectance spectra, and two troughs around 1500 and 2000 nm, both related to strong water absorptions[33], making the snow effectively a black object at these wavelengths.

The differences in snow reflectance of dry snow (Fig. 2) that we observed in our measurements were not possible to be traced back to specific optical characteristics of snow. We were not able to control snow grain size in our measurements, and neither the amount of inorganic impurities or the age and compactness of the snowpack layers that were measured, factors that all are expected to impact snow reflectance[15,34-37].

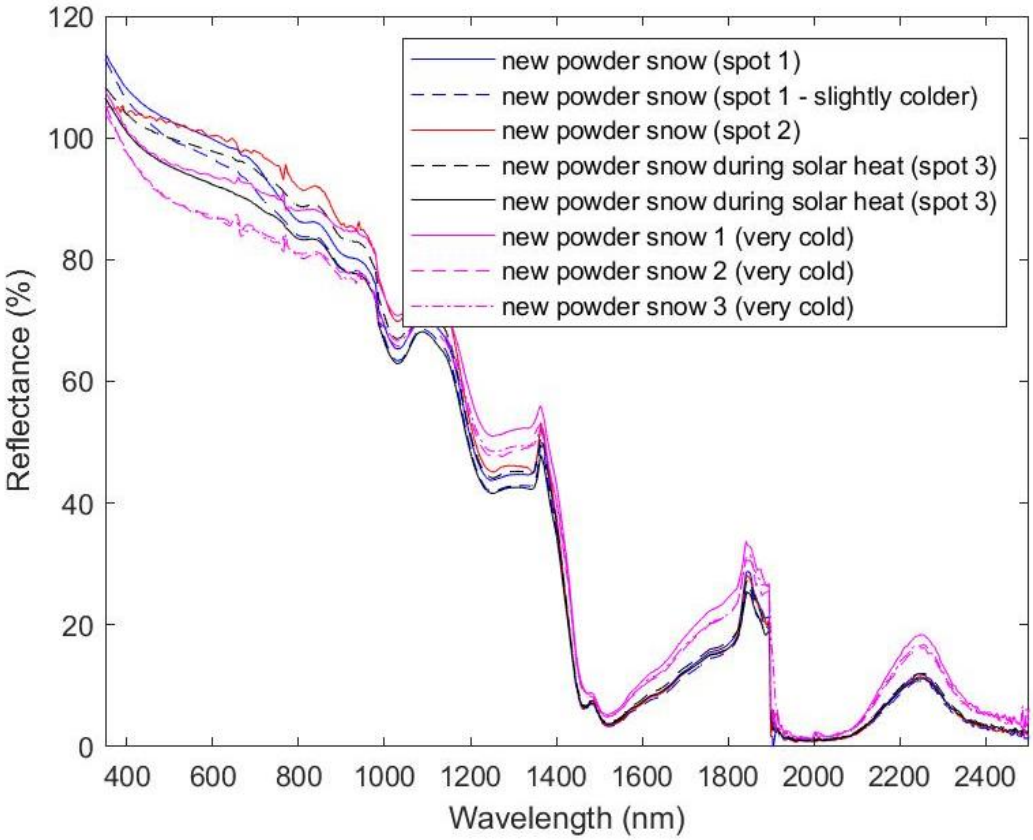

Figure 2. Spectral reflectance of various types of dry, powder snow: Experimental data plotted against wavelength. Snow mass thicknesses measured were 20 cm or more.

Figure 3 shows reflectance spectra of coarse (and cold, dry) snow, i.e. snow that melted and then froze again, one or several times prior to the measurements. Such thawing and freezing is expected to induce changes in snow crystal structures (*i.e.* larger snow crystals[1,2]) relative to new, and dry powder snow. Overall, we note from Figure 3 that the various types of measured coarse snow had similar reflectance spectra. Still, we see that one of the coarse snow types (dotted line - "slightly

Downloaded From: https://www.spiedigitallibrary.org/conference-proceedings-of-spie on 18 Oct 2021
Terms of Use: https://www.spiedigitallibrary.org/terms-of-use

coarse snow") had different shape of the spectra in the lower parts of the visible range relative to the two other types of coarse snow measured.

The coarsest snow type had the lowest reflectance values (solid red line, Figure 3), which is likely due to effects of reduced multiple scattering within a snow layer as the grains become coarser. Coarser snow has been reported to have larger snow crystals, and less air between the crystals (more densely packed, reduced snow porosity) than fine snow[1,2,34]. This means that incoming light is, from the point it starts interacting with the snow, less time in the air "pockets" that exist between the snow crystals (and most prominent for dry powder snow) and more time within the snow crystals themselves (such as coarse snow). As a consequence, the absorption increase, resulted in a reduced reflectance spectra. For wavelength ranges where water absorption is thought to be strong (1250-1300 nm)[33], the difference in reflectance spectra as a function of snow coarseness is found to be particularly apparent, with the very coarse snow reflecting much less light relative to the two other coarse snow types.

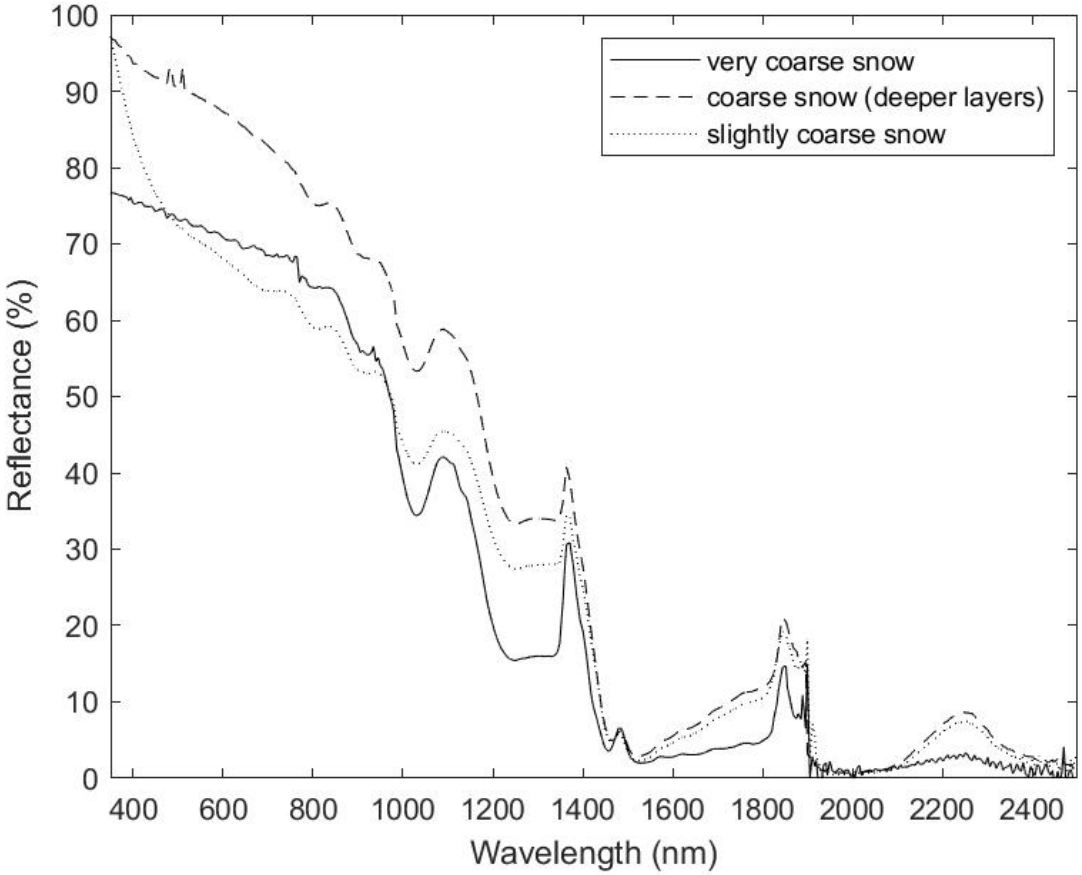

Figure 3. Spectral reflectance of various types of coarse snow: Experimental data on very coarse snow (solid line), coarse snow found in deeper snow layers (dashed line), and slightly coarse snow (dotted line) plotted against wavelength. Snow mass thicknesses measured were 10 cm or more.

Figure 4 presents the spectral reflectance spectra of various types of wet snow, typically ranging from slightly wet snow (dry powder snow exposed to melting temperatures for a few hours) to very wet snow (coarse snow during melting processes that has been exposed to mild temperatures and long, high solar loading during spring time). We see from the experimental results presented in Fig. 4 that all wet snow types had reflectance spectra with the same overall characteristic shapes, albeit with large differences in absolute reflectance values. It seems that the wettest snow (red dotted line, Fig. 4) had the lowest reflection values, while the driest snow (black solid line, Fig. 4) reflected light the most (apart from the visible wavelength range). In the visible range we note the very different reflectance values seen amongst the different wet snow types (varying from about 70 to 100 %), and to some degree different reflectance curve shapes. The very wet snow types (red dotted line, Fig. 4) reflected more light when the wavelength increased from 400 nm to about 600 nm, which was not seen for the other types of wet snow.

Downloaded From: https://www.spiedigitallibrary.org/conference-proceedings-of-spie on 18 Oct 2021
Terms of Use: https://www.spiedigitallibrary.org/terms-of-use

For wavelengths longer than about 1000 nm, and in particular from about 1200 nm and longer, we see that all the wet snow types measured (apart from the slightly wet snow) converge into a narrow reflectance band. This means that all the reflectance spectra became nearly alike given by i) the same reflectance values per wavelength (apart from the blue graph representing wet snow) at about 1370-1390 nm, and ii) by reflectance curve shapes with similar characteristic features. The difference in reflectance spectra between the slightly wet snow and the remaining (and wetter) snow types was more pronounced in this wavelength region, as expected as the interstitial spaces in snow are more filled with water with increasing snow wetness, reducing the reflectance[34]. The wet snow was observed to be very dark (< 20 % reflectance) at 1200 – 1350 nm, whereas the slightly wet snow (black solid graph) was much brighter (> 40 % reflectance).

A similar difference between the wet and less wet snow was seen for wavelength regions at 1500 to 1800 nm, where the driest snow (containing the lowest amount of liquid water) had a markedly increase in reflectance values (from about 5 to 20 %, black graph in Fig. 4), whereas the wet snow reflectance values in the same region were all below 5 %. Hence, it seems that a higher liquid water content (related to snow melting processes) result in a markedly reduction in snow spectral reflectance at 1200 nm and higher.

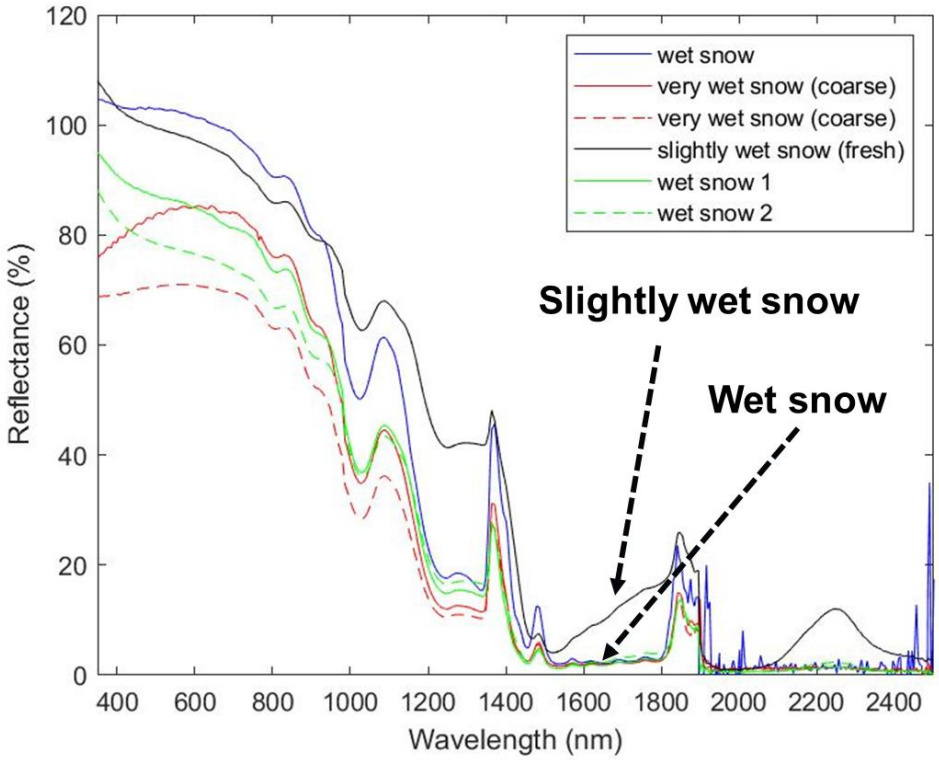

Figure 4. Spectral reflectance of various types of wet snow: Experimental data on very wet snow (red lines), wet snow (blue and green lines), and slightly wet snow (black line) plotted against wavelength. Snow mass thicknesses measured were 10 cm or more.

Figure 5 shows spectral reflectance data for dry snow, coarse snow, and wet snow, allowing direct comparison of spectral features. All snow types had the same overall spectral reflectance curve shapes, yet with differences observed at specific wavelength regions. Dry snow had the highest reflectance for all wavelengths. We observed the wet snow to be slightly more reflective than coarse snow in the visible region. From wavelengths about 900 nm and longer, reflectance curves of wet snow and coarse snow were crossing, making the wet snow less reflective than coarse snow. The wettest snow types measured, presumably containing the highest amount of free “bulk” liquid water, had the lowest reflectance for all wavelengths.

The effect of wetness of snow seemed to affect the measured reflectance, shifting it towards less reflectance values, from approximately 900 nm and longer, which we expect is due to meltwater now filling the interstitial spaces in snow, replacing the air-ice interface with water-ice interfaces. Consequently, light is scattered forward deeper into the snowpack, resulting in a reduction of measured reflectance[34,38]. In addition, stronger water absorption effects for wavelengths in such near

Downloaded From: https://www.spiedigitallibrary.org/conference-proceedings-of-spie on 18 Oct 2021
Terms of Use: https://www.spiedigitallibrary.org/terms-of-use

infrared wavelength regions may affect the reflectance[33]. In some wavelength regions wet snow also seemed to alter the shape of the reflectance curves, and not only the reflectance value levels (Fig. 5). For example, for wavelengths between approximately 1500 and 1800 nm, the wetness level of snow did not only shift the reflectance curves towards lower values, but also altered the reflectance curve shape significantly, with maximal change in shape for the wettest snow.

Furthermore, Fig. 5 shows that the very wet snow had different reflectance curve trend than the remaining snow types tested in the ultraviolet and lower visible region. Changing from dry snow (blue and red lines in Fig. 5) to wetter types of snow (black and red dotted lines in Fig. 5), the plateau observed at 900-950 nm gradually vanished. This probably corresponds to a reported offset in absorption peaks between water and ice or snow[1]. In addition, we observed the variation in reflectance to be maximal at about 1050 nm and in the wavelength range 1250 – 1350 nm, which has also been reported in similar studies[15], and is considered to potentially be due to ageing and grain-size effects[15], and moist levels[34]. Such characteristic snow reflectance variations with snow moist level are thought to be useful in discriminating wet snow from dry snow in remote sensing applications[15,39].

Moreover, reflectance values (Fig. 5) at visible and lower parts of the near-infrared wavelengths were observed to be nearly constant with wavelength (about 400 nm to 850 nm), which has also been observed in similar studies[2], and which might be a consequence of the real part of the index of refraction having little variation with wavelength in this range. This means that reflection coefficients of, in this case, wet snow seemed to be nearly constant with wavelength in the regions visible to the naked eye.

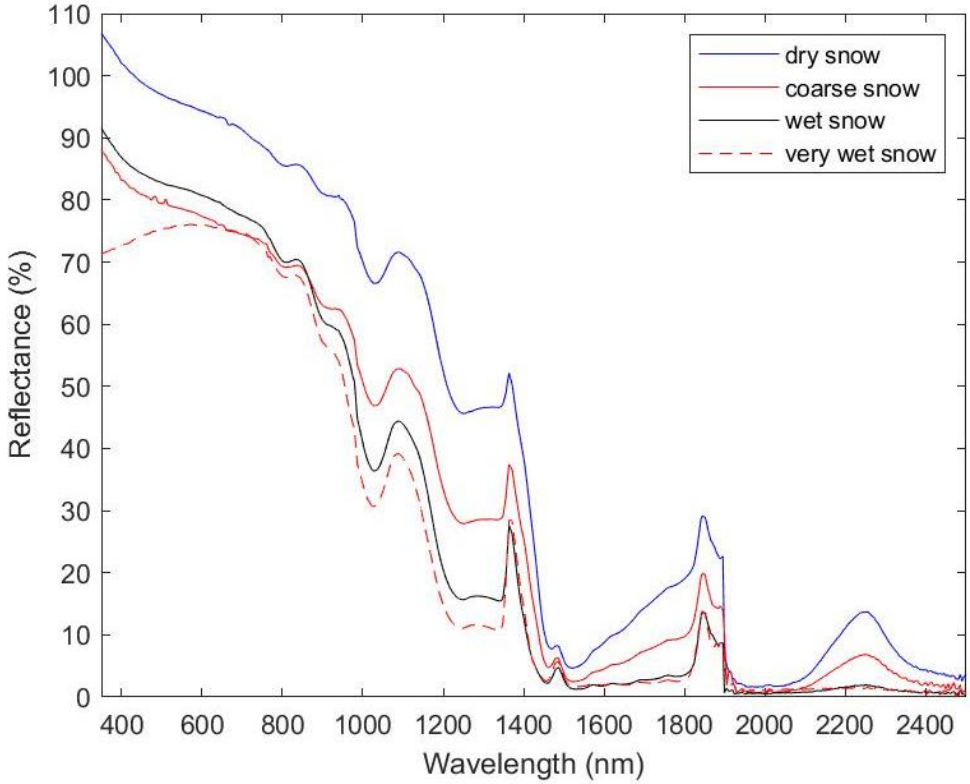

Figure 5. Spectral reflectance data of different types of snow: dry snow (blue solid line), coarse snow (solid red line), wet snow (black solid line) and very wet snow (dotted red line) plotted against wavelength. Reflectance measurements were carried out on snow mass thicknesses of 10 cm or more.

4.2 Snow signatures compared to green vegetation signatures (with and without frost)

Fig. 6 presents reflectance measurements of different types of snow (taken from Fig. 5) compared with similar reflectance measurements on green vegetation. We see that the reflectance spectra of snow and vegetation, including the vegetation that we measured when it was covered in a thin frost layer, were very different in the visual part of the wavelength region, as expected. However, as wavelength regions exceed about 800 - 900 nm, the spectral reflectance differences between

Downloaded From: https://www.spiedigitallibrary.org/conference-proceedings-of-spie on 18 Oct 2021
Terms of Use: https://www.spiedigitallibrary.org/terms-of-use

snow and vegetation were much less apparent, as also reported in other studies[37]. In other words, for wavelengths longer than 900 nm, vegetation starts looking much like snow when integrating reflectance values over certain wavelength ranges.

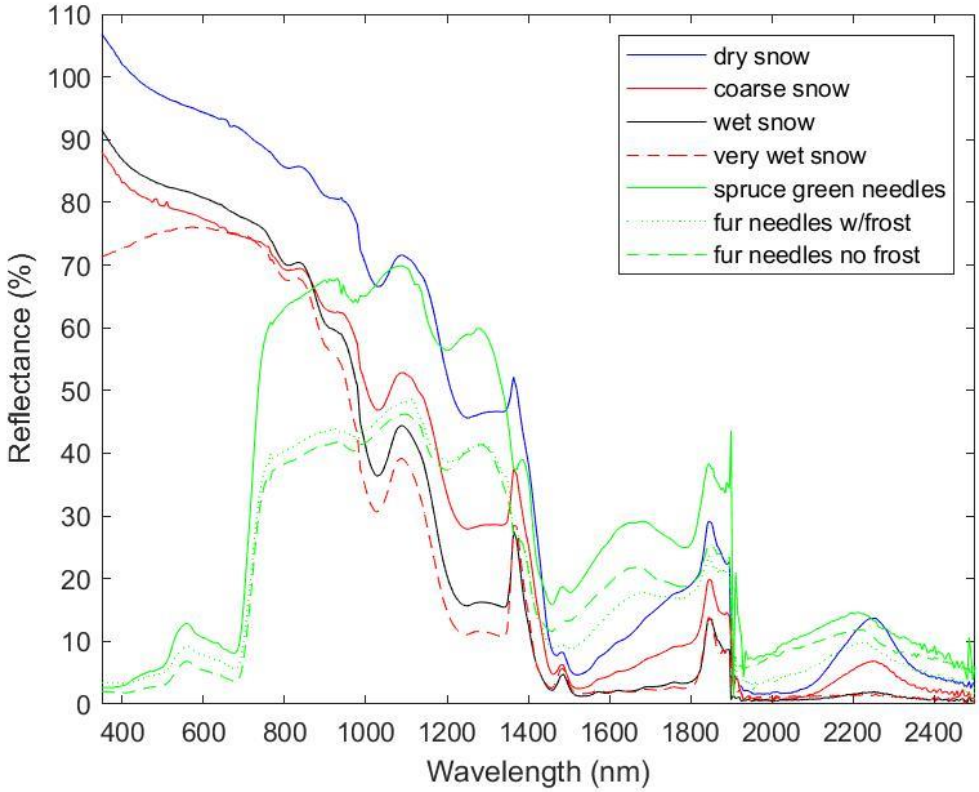

Figure 6. Spectral reflectance data of vegetation, vegetation with frost and snow. The figure shows dry snow (blue solid line), coarse snow (solid red line), wet snow (black solid line), very wet snow (dotted red line), green spruce needles (green line), pine tree needles with frost (dotted green line), and pine tree needles (dashed green line) plotted against wavelength. Reflectance data of snow are as shown in Fig. 5.

Differences in reflectance spectra between snow and vegetation were observed particularly for wavelengths between 1200 and 1300 nm where the vegetation spectra (green lines in Fig 6) had peaks. In the same wavelength range, snow reflectance data did not have a peak, rather a trough-like curve shape, most likely due to strong water absorption[33]. The snow reflectance curves (red and black lines, Fig. 6) had peaks in the spectral curves at about 1350 nm. The corresponding vegetation curve spectra (green lines, Fig. 6) were observed not to have such distinct peaks, but rather less pronounced peaks at slightly higher wavelengths (spruce needles, solid green line, Fig 6) or no distinct peaks (pine tree needles, dotted and dashed green line in Fig. 6). Finally, from 1450 to 1800 nm, all the vegetation reflectance spectra (green lines, Fig. 6) showed similar, though not identical, behavior as the corresponding reflectance spectra of coarse and dry snow (blue and red line, Fig. 6), but had less similarities with the spectral curves of wet snow (black and red dashed line, Fig. 6). A mix of vegetation and snow was not measured, although this is considered very relevant for camouflage purposes as many natural backgrounds of relevance often consist of such a mix.

We also see the effect of a thin frost layer (thickness was not possible to estimate) on the spectral reflectance of green vegetation (pine needle tree). In the visible wavelength region, the frost-covered pine (green dotted line, Fig. 6) had higher reflectance values compared to a corresponding pine with no frost on it (green dashed line, Fig. 6). The spectral curves of pine with frost and no frost differed, starting from the visual range, until wavelengths reached about 1100 nm, the two curves (dotted vs dashed green curves in Fig. 6) were near-identical until approximately 1450 nm. At this wavelength, the two reflectance curves crossed, and for higher wavelengths the pine with frost on it had lower reflectance than pine with no frost (dotted vs dashed green curves in Fig. 6). A similar "cross-over" at 1450 nm, was also observed for similar measurements on green moss with and with no frost covering it (results not shown). Hence, frost covering green vegetation seems to increase reflectance in the visual and near-infrared wavelength ranges (as the frost cover is brighter than the

Downloaded From: https://www.spiedigitallibrary.org/conference-proceedings-of-spie on 18 Oct 2021
Terms of Use: https://www.spiedigitallibrary.org/terms-of-use

underlying vegetation) and decrease reflectance above 1450 nm, an effect we believe is due to water absorption effects as also observed for wet versus dry snow above 1450 nm (see Fig. 5).

4.3 Snow signatures as a function of solar angle

Figure 7 shows the spectral reflectance of coarse dry snow measured at different times throughout the day. The measurements were conducted symmetrically around the time-of-day at which the solar height was maximal (which was about 12:30 p.m. local time) and at the same snow spot for all measurements. The snow was kept in the shadow between measurements to reduce melting effects caused by the sun. We see that the reflectance values captured varied throughout the day for wavelengths of about 350 nm up to 1400 nm, but that all measurements resulted in spectra similar to reflectance spectra for coarse snow and dry snow (cmp. Fig. 5). Similar measurements on a green reference textile did not show the same variation in reflectance spectra as snow as a function of measurement-time during the day (Fig. 8). For higher wavelength regions, little or no differences were observed in the snow spectra (Fig. 7) and textile spectra (Fig. 8). The reflectance values (350 – 1400 nm) were smallest when measured before noon, and were also increasing in this wavelength region as the time-of-day approached 12:30 p.m. where the sun angle was at its highest. Reflectance values (350 - 1400 nm) continued with an increasing trend with time also during the afternoon measurements, as the sun angle was gradually getting lower.

Thus it seems that the variations in snow reflectance (350 – 1400 nm) cannot be due to the variations in solar angle (and hence snow illumination angle) alone. The reflectance measurements were all carried out at angles perpendicular to the snow surface, measuring Lambertian reflection and not specular. It is therefore not clear to us what were the underlying factors contributing to the observed drift in snow reflectance spectra. As the measurement day evolved, the snow was gradually more warmed up by the sun and by the air temperature rising (though not exceeding 0 ºC), and this might have caused changes (thermodynamically induced changes in snow morphology[11]) in the snow structure affecting the reflectance. As any proper explanation are not possible to draw from the measurements, further studies are required.

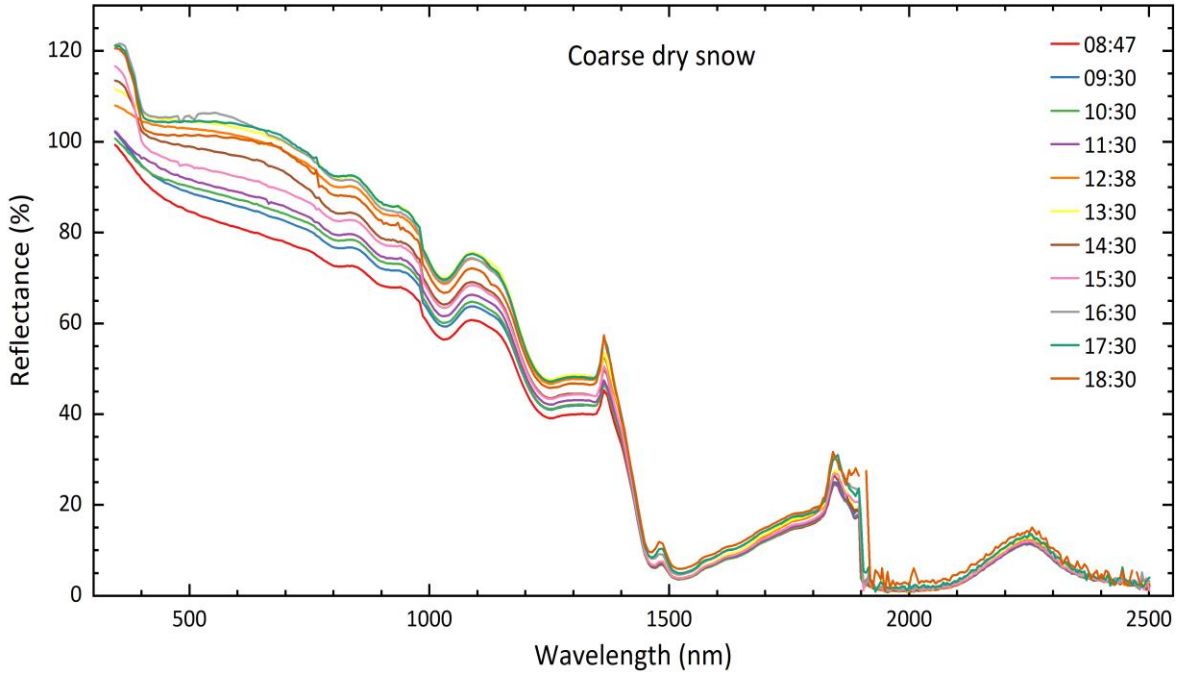

Figure 7. Spectral reflectance measurements of coarse, dry snow at different time-of-day, corresponding to different solar incident angles.

Downloaded From: https://www.spiedigitallibrary.org/conference-proceedings-of-spie on 18 Oct 2021
Terms of Use: https://www.spiedigitallibrary.org/terms-of-use

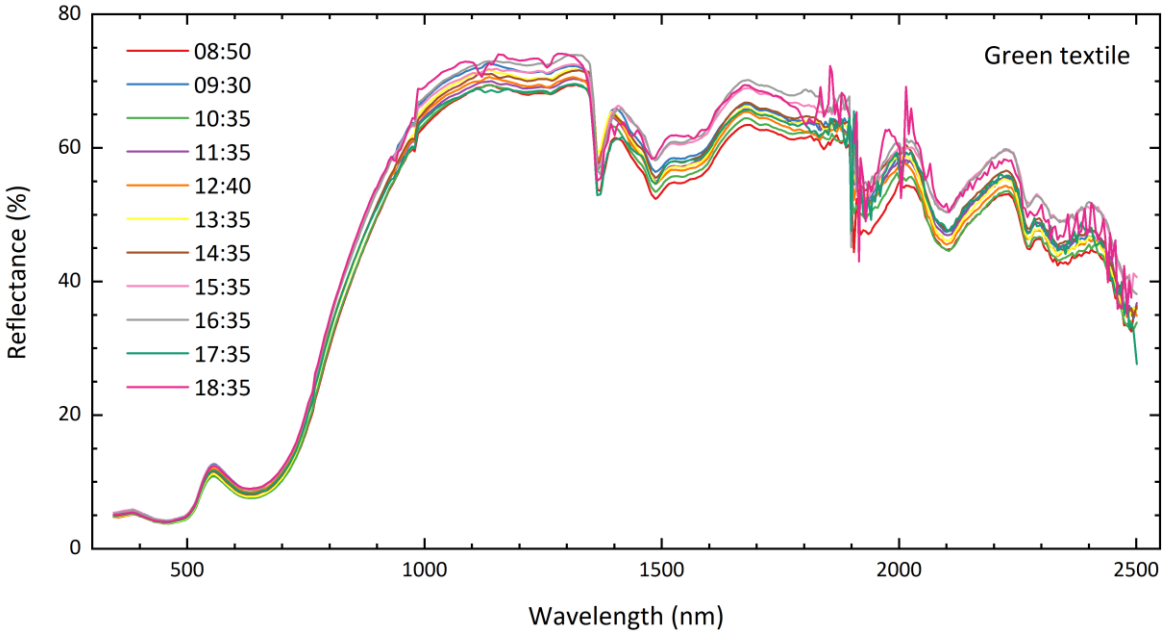

Figure 8. Spectral reflectance measurements of a green reference textile at different time-of-day, corresponding to different solar incident angles. The reflectance measurements of the green textile were conducted under identical conditions as the measurements on snow shown in Fig. 7.

5 RESULTS PART TWO – MEASUREMENTS OF REFLECTANCE OF SNOW AS FUNCTION OF LAYER THICKNESS (SNOW MASS PER UNIT AREA)

In this section, we present experimental results from reflectance measurements of snowpack layers of various thickness when placed on top of an underlying object (synthetic, green textile material) for wavelengths in the region 350 – 2500 nm.

5.1 Measurements of reflectance of snow as function of layer thickness (snow mass per unit area)

Figure 9 shows experimental data from measurements of spectral reflectance of snowpack layers of different thicknesses, on top of a green textile. The snow used for the measurements was wet and coarse (corresponding to the very wet snow in Fig. 5, dotted red line) and the textile was wetted due to the high wetness levels of the snow soaking the underlying textile. Figure 10 shows images of the different snowpack layers used during the measurements. We see from Fig. 9 how the spectral reflectance of a green textile sample (dotted green line) is altered as snow layers are accumulated on top of it, starting from 0.55 cm (solid red line) and exceeding 11 cm (dashed purple line). At the thickest snowpack values (> 11 cm) we see that the experimental snow reflectance data were approaching the inherent spectral characteristics of wet, coarse snow (*by for example comparing* the dashed purple line in Fig. 9 with the dashed red line in Fig. 5). Furthermore, we note that the impact of variations in snowpack layer thicknesses on the spectral reflectance measured were not the same over all wavelengths, but rather varying much depending on which wavelength region that is being considered. As there were large differences in how the snowpack thickness affected the spectral reflectance in the visible, near-infrared and short-wave infrared regions, we discuss these in further detail in Section 5.2 to 5.4.

Downloaded From: https://www.spiedigitallibrary.org/conference-proceedings-of-spie on 18 Oct 2021
Terms of Use: https://www.spiedigitallibrary.org/terms-of-use

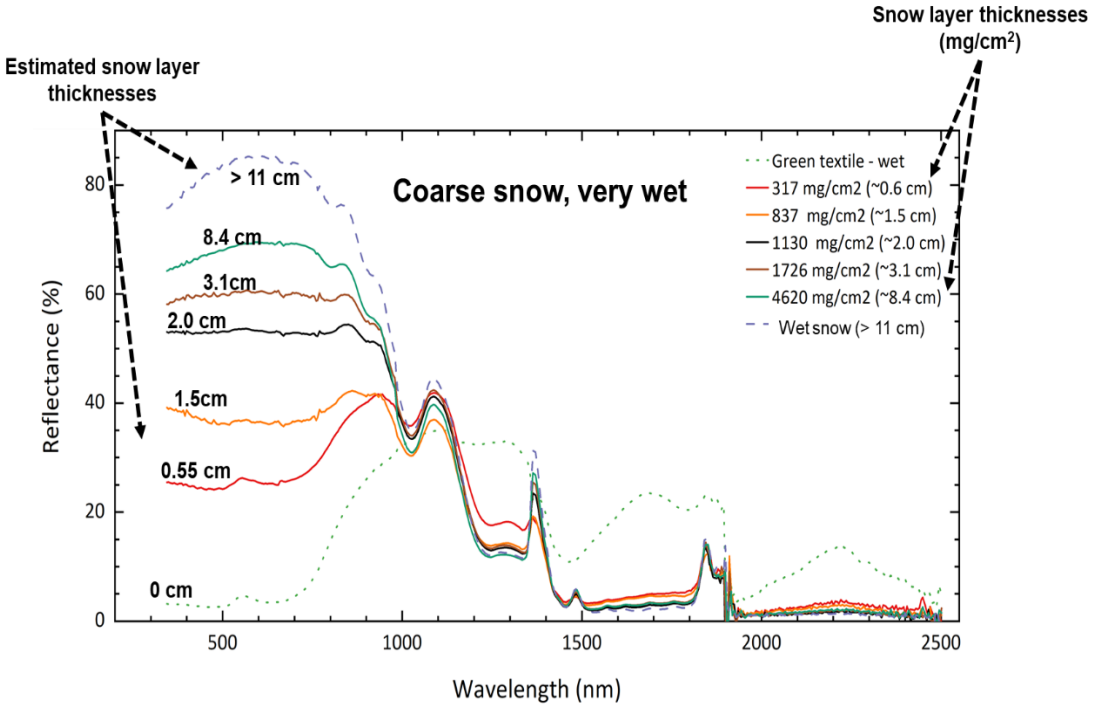

Figure 9. Spectral reflectance data for a green and wet textile sample (dotted green line) as a function of snowpack layer thickness and wavelength. Snow layer thickness is given as mass per area (mg/cm2) and is converted to estimated snow layer thicknesses (cm).

5.2 Effects of snow thickness on reflectance – visible and near-infra red region

Figure 10 shows close-up results of the graph shown in Fig. 9, now focusing on the visible and near-infra red regions. We note that the (wet) snow seemed to be much more transparent in the visible region and in the lower parts of the near-infrared (500 – 850 nm) than for wavelengths above 850 nm. This is seen as a snow layer of up to 8 cm was needed in the visible range until the reflectance curves of snow (and green textile underneath it) resembled that of pure (wet) snow. In the near infra-red region (> 850 nm), however, a (wet) snow layer of 2-3 cm thickness seemed to be sufficient to establish a near-identical reflectance curve similar to that of pure snow (shown in Fig. 9), as also indicated in other studies[15].

The digital images shown to the right in Fig. 10 illustrate the visual impression of the results shown in the corresponding reflectance curves (left in Fig. 10). We note the overall trend that the sample (textile and snow combined) appears whiter with increasing snowpack thickness up to thicknesses of more than 8 cm. Furthermore, we see that snow layers thinner than about 1 cm did not appear to have uniform thickness over the snow sample area, but rather appeared as a macro-porous structure with holes penetrating down to the textile at some point. It was our experience that the wet and coarse snow type that was used for snow layer sample preparations was difficult to distribute evenly in the thinnest layers, as it was sticky and clustering into larger snow lumps. Yet being very thin, transparent and with holes in it, we note that the thinnest layer of snow used (0.55 cm, red solid graph in Fig. 10) significantly altered the signature of the underlying object (green dashed line), albeit to some other signature than pure, wet snow.

As the incident light approaches near infra-red regions (< 750 nm) we see from Fig. 10 that the reported offsets[1] in plateau (940 nm) and valley (1030 nm) are affected by thinner snow layers and presumably the increased influence of the underlying object on the measured spectral signatures. As the snow layers were thinner, the negative gradient for wavelengths above the plateau (< 940 nm, and in particular from about 970 nm) got shallower and the valley at 1030 nm seemed to be less distinct when the effective snowpack thickness was reduced. As liquid water is known to have a water absorption line at 970 nm[33], a thicker layer of wet snow, effectively increasing the water layer thickness incoming light interacts with, is likely to yield a more rapid reduction in reflectance (increase in absorptance) at the absorption lines. We discuss further results of the near-infrared spectral characteristics in section 5.3.

Downloaded From: https://www.spiedigitallibrary.org/conference-proceedings-of-spie on 18 Oct 2021
Terms of Use: https://www.spiedigitallibrary.org/terms-of-use

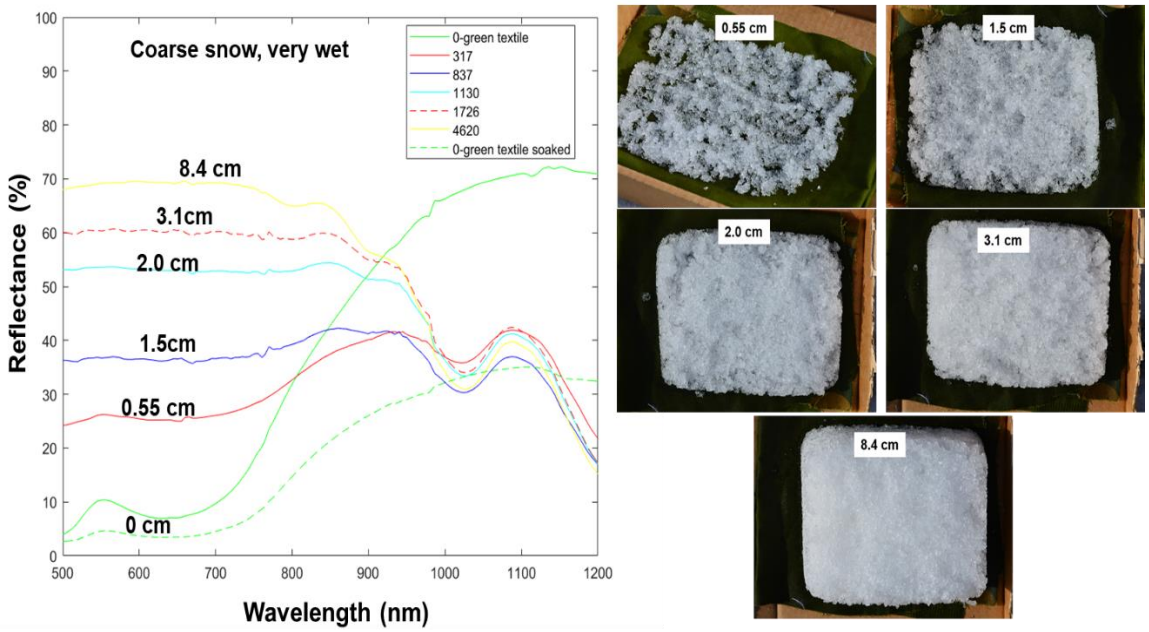

Figure 10. Effect of snow layer thickness on reflectance in the visible and near-infra red regions. Left: Spectral reflectance data for a green and wet textile sample (dotted green line) as a function of snowpack layer thickness and wavelength. The solid green line shows the spectral reflectance of the green textile initially, before it was soaked. Snow layer thickness is given as mass per area (mg/cm2) and has been converted to estimated snow layer thicknesses (cm). Right: Corresponding digital top images taken of the snowpack layers on top of a green textile.

It is also interesting to note (Fig. 10) that (wet) snow coverages seem to be less effective to mask the signature of an underlying object, for a given mass per area (effectively meaning layer thickness), compared to natural biomaterials such as thin, semi-transparent, leaf structures (leaves found in canopies). We found that 10 or more centimeters (visual region) and 2-3 centimeter (near-infra red) was needed for a (wet) snowpack layer to mask the underlying object. Leaves, such as from birch and oak, on the other hand, only required about 0.3 mm (corresponding to 2-3 stacked layers of leaf material) to conceal an underlying object in the visual region, and about 1 mm (7-8 stacked leaf layers) in the near infra-red region[14]. Consequently, the high degree of porosity of snow, being a mix of ice and water, makes it much more transparent, given by effective thickness, than thin leaf-like biomaterials, particularly in the visible wavelength region.

5.3 Effects of snow thickness on reflectance – near-infra red and short wave infrared

Figure 11 presents the experimental results of the snow signature measurements in the wavelength region 1000 – 1200 nm. As an overall trend, all the snow layer thicknesses resulted in reflectance values that converged into a relatively narrow band. A likely explanation is that the soaked green textile itself (green dashed line) had this signature in this wavelength region. Measured reflectance values may therefore be due to free water effects as we see that the green textile, when dry (green solid line), achieved much higher reflectance values than any of the combinations of wet snow on top of a wet green textile.

As the spectral signature of the underlying reference material (soaked green textile) and the corresponding reflectance signatures of the various snow layers were much more similar in this wavelength region than in the visible range, it was more difficult and uncertain to find the effects of snowpack thickness on the spectral signature. This wavelength region was also the region with the poorest fit of experimental data to a model of light reflectance in thin, semi-transparent materials (see Section 5.5, Fig. 13). A reported water absorption line of increasing size at 1200 nm[1] is potentially explaining that the thickest snow layer (yellow line), i.e. containing more absolute liquid water per sample area, had the lowest reflectance value at 1200 nm, whereas the thinnest snow layer (red line) had the highest reflectance at this wavelength.

Downloaded From: https://www.spiedigitallibrary.org/conference-proceedings-of-spie on 18 Oct 2021
Terms of Use: https://www.spiedigitallibrary.org/terms-of-use

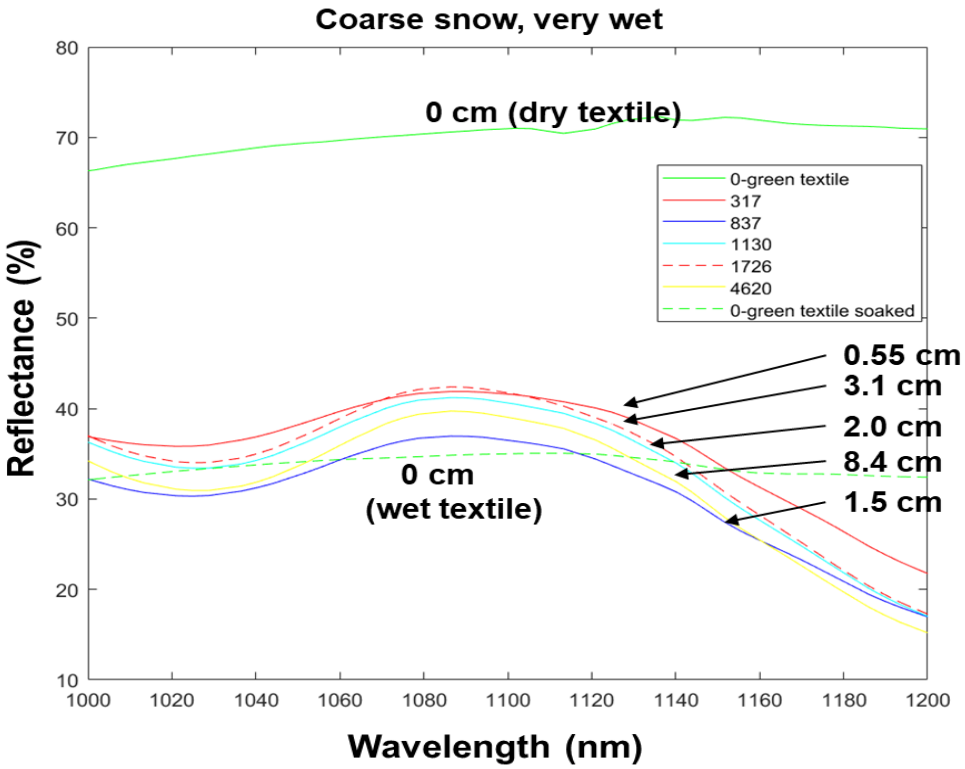

Figure 11. Effect of snow layer thickness on reflectance in the (upper) near infrared region. Spectral reflectance data for a wetted green textile sample (dotted green line) as a function of snowpack layer thickness and wavelength. The solid green line shows the spectral reflectance of the green textile initially, before it was soaked. Snow layer thickness is given as mass per area (mg/cm2) and has been converted to estimated snow layer thicknesses (cm).

5.4 Effects of snow thickness on reflectance – short wave infrared (above 1300 nm)

Figure 12 shows the spectral reflectance data of various snowpack thicknesses (covering a wet textile) in the wavelength region 1300 – 1500 nm. As we also saw from the measurements of different snow types (Fig. 5), the different snow layers achieved very low reflectance values in this wavelength region (apart from a local peak at 1350 – 1400 nm). Between 1300 and 1350 nm the thickest of the wet snow layers (yellow line) had the lowest reflectance value with values around 12 %, whereas the thinnest layer (red line) had a markedly higher reflectance of about 17-18 % which is likely to be due to the green textile (green dashed line) affecting the measured reflectance.

The snow layer thickness needed to resemble the observed peak in reflectance around 1370 nm (higher reflection values with increasing snow layer thickness), was observed to be exceeding ca. 2 cm (turquoise line), and surely thicker than the thinnest layer tested (0.55 cm, red line). The distinction in signatures (green sample and wet snow on top) with increasing snow layer thickness seemed to be more present in this wavelength range (1300 – 1500 nm) than at 1000 – 1200 nm (Fig. 11). Furthermore, the lowest reflectance values were observed at about 1450-1460 nm, and no significant difference amongst the snow layers of different thicknesses were seen, which fits reasonably well with liquid absorption to be reported to peak at about 1450 nm[1]. We also note (Fig. 12) the large difference in reflectance between a dry textile (green line) and a similar, but wet, textile (dashed green line) which is due to water absorption effects in this wavelength region[14].

Downloaded From: https://www.spiedigitallibrary.org/conference-proceedings-of-spie on 18 Oct 2021
Terms of Use: https://www.spiedigitallibrary.org/terms-of-use

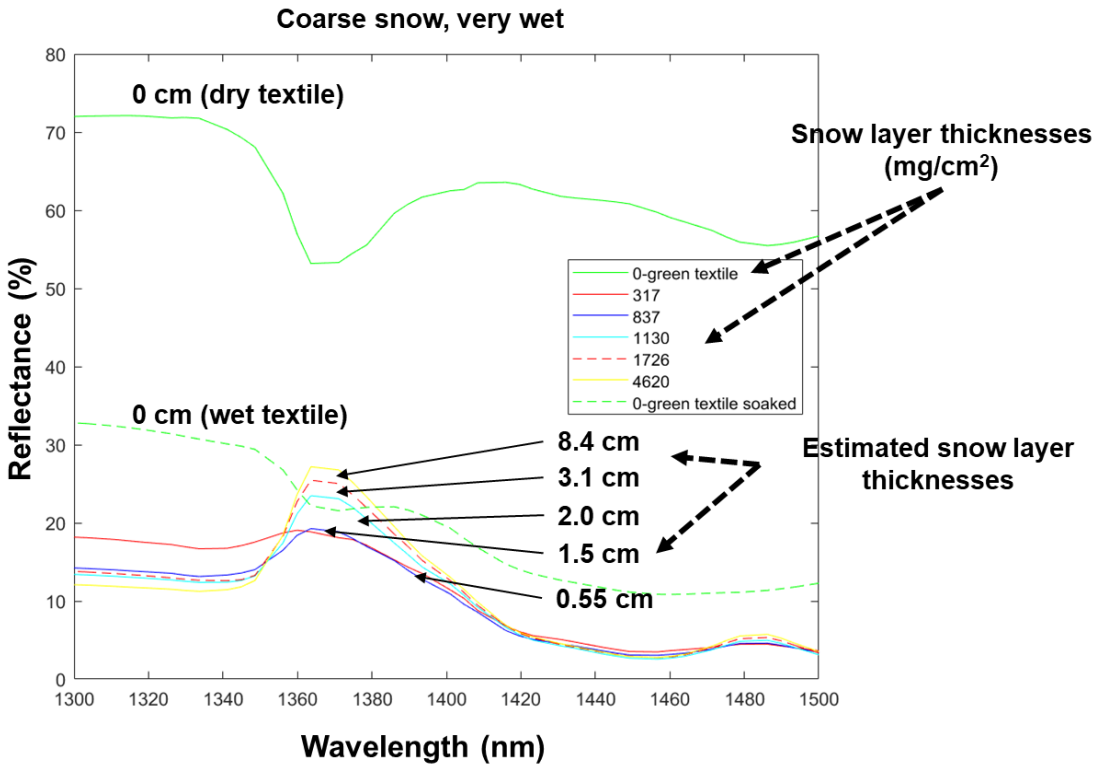

Figure 12. Effect of snow layer thickness on reflectance in the short-wave-infrared regions. Spectral reflectance data for a wetted green textile sample (dotted green line) as a function of snowpack layer thickness and wavelength. The solid green line shows the spectral reflectance of the green textile initially, before it was soaked. Snow layer thickness is given as mass per area (mg/cm2) and has been converted to estimated snow layer thicknesses (cm).

5.5 Discussion of the effects of snow thickness on the measured reflectance

The results presented in Fig. 9 – 12 confirm some of the expected assumptions that objects located underneath a snow layer may be detected by an observer or sensor. The degree of detectability depends on both wavelength region and thickness of the snowpack layer. We found that incoming (solar) light in the visible region was more likely to penetrate a wet snow layer (of a given thickness), hit the underlying object and then be reflected back through the snow layer, reaching an external sensor, such as the human eye. Snow layer thicknesses of 10 cm or more (Fig. 9 and 10) were needed to effectively hinder the underlying object in contributing to the measured signature. In the near infrared wavelength regions (> 800 nm), however, the amount of light reflected back (through the snow layer) from the object was significantly less than in the visible region and snow layer thicknesses of about 2 cm of wet snow was found to be sufficient to attain most of the pure snow reflectance characteristics. Hence, it seems that only smaller amounts of the incoming light was transmitted in the near-infrared wavelength regions (transmittance was not measured in this study).

For camouflage purposes, we see that the spectral reflectance (including the color appearance of any observer) of a hidden object similar to the (wetted green) tested, will be different from a pure (and thick) snowpack layer up to layer thicknesses of about 8 cm in the visible region. Green objects covered with thinner snow layers will appear darker than the snow, and become gradually darker as the snow layer thickness is reduced, when viewed from any external observer. Incoming light in the visible region will be gradually attenuated by the snowpack layer until little light is reflected back from underlying object, through the snowpack, back to the sensor, when the snowpack is sufficiently thick (about 12 cm in this study). Until the snowpack is sufficiently thick, there is an increased risk that the object will not look like snow, but generally as a darker object (or even brighter if the object is more reflective than snow at the given wavelength). This means that information received by a sensor in the visible wavelength bands is more likely to be a mix of snow signatures and object signatures than in the wavelength regions exceeding the visible.

Downloaded From: https://www.spiedigitallibrary.org/conference-proceedings-of-spie on 18 Oct 2021
Terms of Use: https://www.spiedigitallibrary.org/terms-of-use

In the near infrared wavelength regions (> 800 nm) the wet snowpack layer seemed to be more effective in masking underlying signatures as the snow transmittance was less affected by variations in snow layer thickness. The first 2-4 centimeters of snow in this wavelength region will constitute effective concealment of an underlying object as the incoming light is sufficiently attenuated in such thicknesses of wet snow. Most near infrared reflectance signatures that are captured (e.g. by a sensor) therefore seemed to be more dominated, by the top centimeters snow layers of a hidden object or placed under snow-covered vegetation or similar. Still, we want to underline that in our experiments, the spectral signature of the underlying object (wetted green textile) and snow signatures were less different in the near-infra red region relative to the corresponding signatures in the visible range. This makes the estimations of light penetration depths in the near-infra red wavelength ranges more uncertain than the corresponding estimations in the visible range.

The observed differences in snowpack penetration depths of incident light are most likely due to i) wavelength effects and ii) and differences in effective thickness of the snowpack. The differences are expected to be of relevance for remote sensing applications where snow (or ice) covered areas are mapped and classified on a continuous basis, particularly for climate monitoring purposes[24,25,34,38], and where differences in red light reflectance and corresponding NIR light are used as spectral snow classification indices[37,38]. Finally, it is known that liquid water has absorption peaks around 970, 1200 1450, and 1950 nm[33], which corresponds well with many of our observations for wet snow (Fig. 9 and 5).

Little has been reported on snow transmission measurements in previous studies, although some studies have been conducted in the visible region and lower near infrared[2,27,30,31]. Snow transmittance measurements have been reported, for wavelengths between 400 and about 1000 nm, earlier[2,30], where snow was found to have a strong wavelength dependent transmittance (maximum at 500 nm, then falling off rapidly with increasing wavelength). Our experimental data show the same tendencies where 10 cm or more (visible region) and 2-4 cm (near infrared) of wet snow was needed to reduce effects of an underlying object on the measured spectral reflectance.

5.5 Spectral extinction coefficients of snow at selected wavelengths

The extinction coefficient, *k*, of snow is an interesting snow material parameter as it states how rapid incoming light is attenuated in a snow layer. The extinction parameter is normally wavelength-dependent and related to transmittance. As snow transmittance is interesting for many purposes (camouflage, land mapping, ice mapping, solar energy harvesting and other), yet very difficult to measure directly, it would be particularly useful if extinction coefficients can be estimated from the extinction model and reflectance measurements alone. A possible interpretation of increased extinction coefficient values is to think of it as an increase in incident light absorptance for a fixed mass per unit area of the material sample. That is, the corresponding transmission decreases fast with an increase in mass per area (which effectively means a thicker snowpack layer).

We used the extinction model (Ch. 3) to estimate extinction values, *k*, at some selected wavelengths (550, 1100, 1300, and 1700 nm) where the snow reflectance responded differently to changes in layer thicknesses (Fig. 9). The wavelengths we selected for further inspection represent different sensor bands, e.g. in remote sensing applications, and different physics regarding for example the influence of water on the measured reflectance. Our experimental data were fitted to the extinction model (Eq. 5–7). The fitting parameters of the model are the extinction coefficient, k and the sample reflectivity, α describing reflectance characteristics of a sample when the thickness is very large.

Figure 13 shows the experimental data fitted to the model, yielding the individual extinction coefficients of wet and coarse snow for the wavelengths 550, 1100, 1300, and 1700 nm. The extinction coefficients are all given in terms of cm^2/mg. For incoming light at 550 nm, we see that the extinction model fitted well with the spectral reflectance data of the wet snow (Fig. 6 (a)). At 550 nm, we see that as the snow mass per area (i.e. the effective snow layer thickness) was increased, the corresponding reflectance seemed to approach a plateau level. This corresponds well with what we would expect since a sufficiently thick snow layer (on top of any underlying object) eventually will have to start looking like pure snow. From our results in Fig. 6 (a), we see that the data fitted to the extinction model converged to a plateau (i.e. stable reflectance values, no longer increasing if additional snow is added to the layer) at about 5000 mg/cm^2. A snow layer that thick can be interpreted as the snow reflectance threshold value. For wet and coarse snow, as investigated in this study, this corresponds to an effective snow layer thickness of approximately 9 cm. The snow reflectance threshold value, defined by us as $R(\lambda)$, will depend on wavelength and we also expect it to depend on several parameters related to snow structure such as grain size, wetness/degree of free water, and so on.

For snowpack layer thicknesses larger than the reflectance threshold value, reflectance will no longer be much affected by any signature of an underlying object. Consequently, being able to estimate the extinction coefficients for different snow types at most wavelengths will be a very useful tool in knowing how much light is being reflected transmitted and absorbed

Downloaded From: https://www.spiedigitallibrary.org/conference-proceedings-of-spie on 18 Oct 2021
Terms of Use: https://www.spiedigitallibrary.org/terms-of-use

by snow for all thickness levels. It will be of high value to know more on what amount of light is reflected back from an object, and towards a remote sensor, or transmitted through to a photovoltaic solar cell. Not only for camouflage purposes, but also for land and sea mapping as well as for solar energy harvesting purposes in areas where snowfalls can normally be expected[27].

The extinction coefficients at the other three selected wavelengths (Fig. 13 (b)-(d)) did not show the same trend as seen at 550 nm. Apart from the coefficient values all being larger than at 550 nm, the fitted curves were different in shape (from that of 550 nm) and near-constant (1100 nm) or slightly decreasing (1300 and 1700 nm) with snow mass per area (effective snow thickness). The difference in curve shapes (increasing or decreasing reflectance with snow mass per area) is most likely due to the underlying object being darker (at 550 nm) and of similar or higher brightness (1100, 1300, and 1700 nm) relative to the inherent snow reflectance.

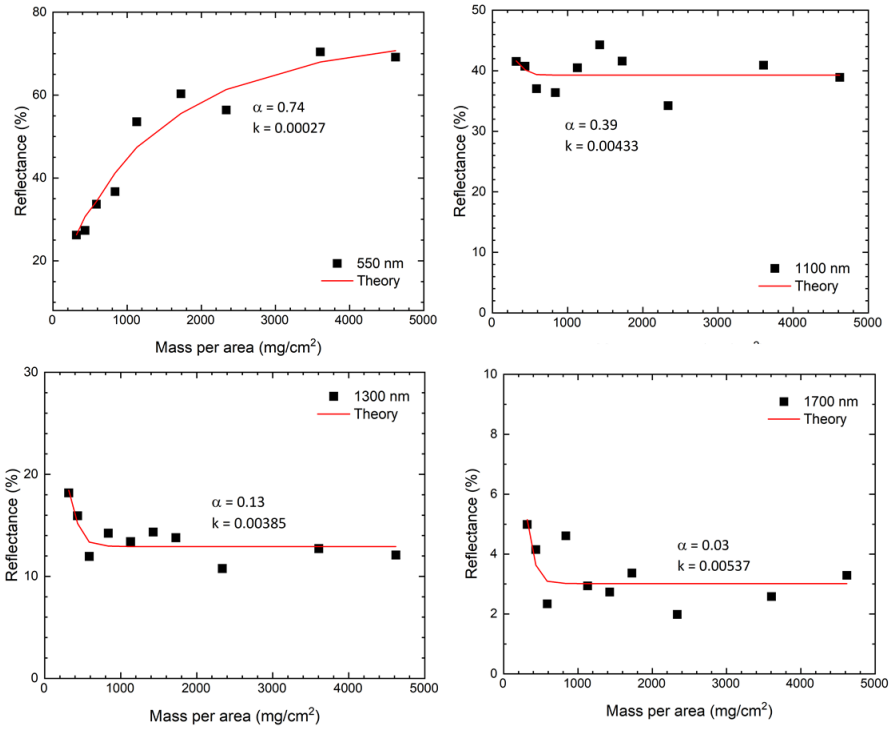

Figure 13. Spectral reflectance properties vs. mass per area for wet snow at (a) 550 nm, (b) 1100 nm, (c) 1300 nm, and (d) 1700 nm. The data points are fitted to the extinction model with different reflectance coefficients (α) (1 equals 100% reflectance, while 0 represents 0% reflectance) and extinction coefficients(k) with dimension cm2/mg.

5.4 Result trends and interpreting the physical meaning of the extinction coefficients

As the extinction coefficients are usually derived from transmission measurements, and as transmission measurements of snow are exceedingly complicated, little has been reported on extinction coefficients of snow[2,31]. Perovich has reported on extinction coefficients for snow up to 900 nm, and found it to increase with snow density and wavelength[2]. If we convert the extinction coefficient values, *k*, in Fig. 13 so that they are of the same dimension as those reported by Perovich (our *k*-values multiplied by 1000 times snow mass density), our extinction coefficients are given as 0.15, 2.41, 2.15, 2.99 (all given in terms of 1/cm) at the four wavelengths 550, 1100, 1300 and 1700 nm, respectively. The corresponding values for Perovich, based on direct transmission measurements, for wet snow were reported between 400 and 900 nm to be approximately 0.2/cm (550 nm to 700 nm) and 0.5/cm (900 nm), and to be rapidly increasing from about 700 nm[2]. Our estimated values of the extinction coefficient, derived by reflectance measurements alone (and not transmission measurements), correspond well with the reported values in the visible region. In the higher near infrared wavelength region (> 900 nm) we have not found dedicated studies that report on extinction coefficient values for snow, although some findings been reported[27,30]. Thus, our estimated values for the extinction coefficient at 1100, 1300, and 1700 nm are, to the best of our knowledge, novel and not possible to compare with other studies.

Downloaded From: https://www.spiedigitallibrary.org/conference-proceedings-of-spie on 18 Oct 2021
Terms of Use: https://www.spiedigitallibrary.org/terms-of-use

We note, however, that the estimated extinction coefficients at 1100 nm and higher (Fig. 13 (b)-(d)) were much higher than for 550 nm (Fig. 13 (a)), and much higher than those reported in the literature at 900 nm (0.5/cm at 900 nm by Perovich[2]). Based on the overall impression given in Fig. 9, any such markedly increase in snow extinction parameters seems to correlate well with our experimentally obtained reflectance data, although it is not possible to verify the extinction coefficient values directly from our data. In Fig. 9, we see that the underlying (and visually much darker) object influenced reflectance data in the visual region until snow layer thicknesses were much larger than the corresponding thicknesses at 1300 and 1700 nm (where the underlying object was brighter than snow). A reduced sensitivity to the underlying object's (inherent) reflectance on the measured reflectance of object and snow combined as the snow layer thickness is reduced gradually, generally imply a higher extinction coefficient.

For wavelengths at 1100 nm, we see from Fig. 9 that the reflectance of the underlying object (wetted green textile) itself was close to the snow reflectance. Such a reduced difference in spectral reflectance of snow and underlying reference object makes it more difficult to derive extinction coefficients from reflectance measurements. Consequently, we expect the extinction coefficient at 1100 nm to be of higher uncertainty than those at 550, 1300, and 1700 nm.

Figure 14 shows data from spectral reflectance data of snow at different layer thicknesses on top of the wetted green textile, and with extinction coefficients marked for the four wavelengths 550, 1100, 1300, and 1700 nm. Apart from the extinction coefficient estimated for 1100 nm (which is considered to be the most uncertain *k*-value), we note the apparent correspondence between extinction coefficient values and how rapid the reflectance data converged to stable values (i.e. towards inherent snow reflectivity at the given wavelength) as the snow layer thickness was gradually increased. At 550 nm the extinction coefficient was 0.15/cm (low) and the corresponding reflectance curves converge slowly towards inherent snow reflectivity (not achieved until > 10 cm layer thickness). At 1300 and 1700 nm wavelengths, however, the extinction coefficients were 2.15/cm and 2.99/cm (both considered high) and the corresponding reflectance curves converged much more rapidly towards stable values as a function of snow layer thickness increments.

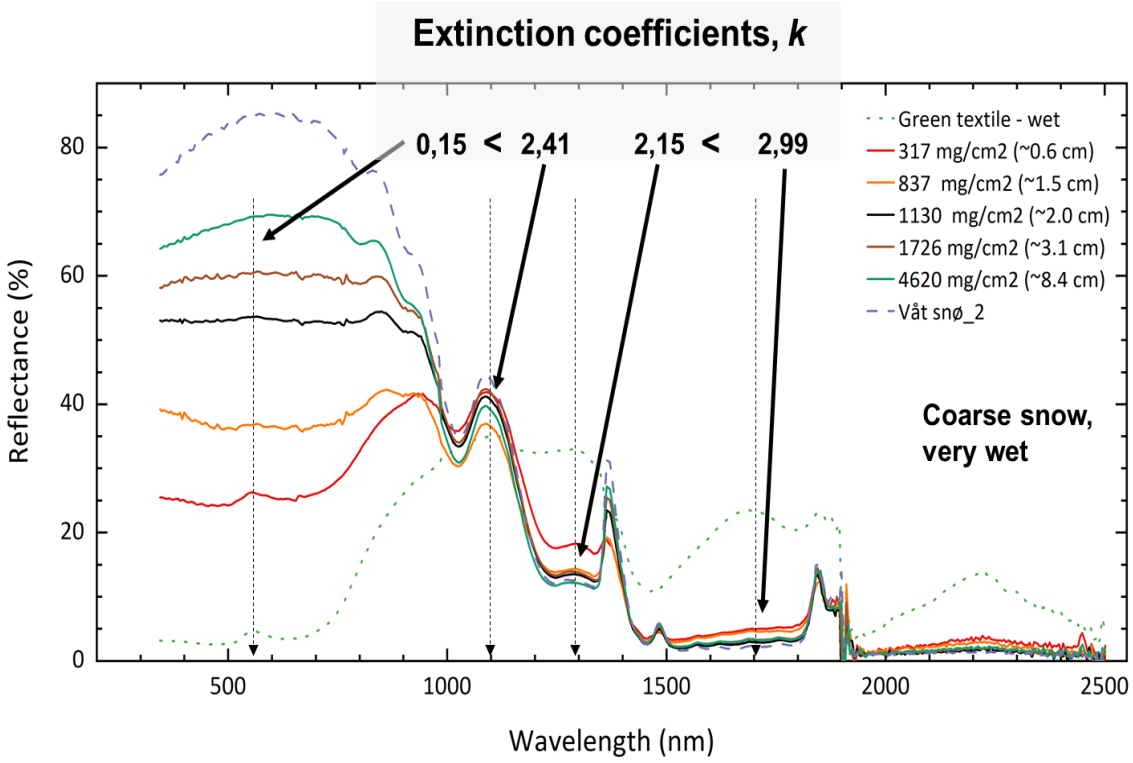

Figure 14. Graphical interpretation of the snow extinction coefficient, k: Spectral reflectance of coarse and wet snow (on top of a wetted green textile) for different snow layer thicknesses. Extinction coefficient values, k, for wavelengths at 700 nm, 1100 nm, 1300 nm, and 1700 nm are given to show that enhanced k-values result in more rapid collapse of snow reflectance curves with increased snow layer thickness.

Downloaded From: https://www.spiedigitallibrary.org/conference-proceedings-of-spie on 18 Oct 2021
Terms of Use: https://www.spiedigitallibrary.org/terms-of-use

7 CONCLUSIONS AND FUTURE WORK

In this paper, we had two primary goals. Firstly, we wanted to study measurements of spectral reflectance on snow, vegetation, frost, and depth-effects of snow coverage on reflectance. Secondly, we wanted to investigate the applicability of a mathematical model used in a predicative sense, providing answers to problems not solvable through direct measurements of inherent (snow) optical properties.

Through our investigations we found that several snow types (fresh powder snow, wet snow, coarse snow, and deep (and older) snow layers) had similar reflectance spectra overall, albeit with noticeable differences. Fresh powder snow reflected more light than wet, older or coarse snow, which all had lower reflectance values. All snow types reflected light distinctly different from vegetation (and frost-covered vegetation) for wavelengths below about 1000 nm. For longer wavelengths, however, the differences between inherent snow reflectance and green vegetation were less pronounced, as all samples showed signs of water absorption effects in the reflectance spectra. Finally, the reflectance of frost-covered vegetation deviated from pure vegetation, but to a much lesser degree than from pure snow.

The snow layer thickness needed to mask a green underlying reference surface was obtained for wet and coarse snow, in specific. Through our measurements, we found the characteristic thickness (corresponding to specific weights of snow per area) needed to effectively hide the spectral reflectance signature of the underlying object. Snow was much more transparent in the visual range (up to about 900 nm), where 10 cm or more was needed to effectively mask the object. For higher wavelength regions, the corresponding snow layer thicknesses were less than halved. Extinction coefficients, which are material parameters describing light penetration in the snow pack, were estimated for wavelengths at 550, 1100, 1300, and 1700 nm by applying our experimental reflectance data to a mathematical extinction model[4,13,16].

Our results further show that the extinction coefficients, obtained by combining reflectance data and modelling, were comparable to extinction coefficient values conducted in earlier studies, based on snow transmittance measurements for wavelength regions 400 – 900 nm. In this study, we have estimated snow extinction coefficients up to 1700 nm, but have not found other reports on snow extinction coefficient for wavelengths exceeding 1000 nm. As transmittance measurements of snow are considered to be difficult to conduct[2,34], our approach - where extinction coefficients can be estimated through precise reflectance measurements and modelling - seems promising. Knowledge of snow extinction coefficient full spectra will further allow for calculations of snow transmittance and absorptance as a function of wavelength.

The effects of a snow layer thickness (covering an underlying object) on the measured reflectance are expected to be useful when camouflage material or camouflage strategies in snow-covered landscapes are developed. In addition, the variation in snow reflectance amongst different types of snow must be taken into account when camouflage material is developed or selected for specific areas. The reported similarities and differences in reflectance properties between snow and living vegetation can be useful for camouflage purposes in areas consisting of a mix of snow and all-year green conifers [9,13,40]. The amount of light penetrating different types of snow and then returning to an external sensor, at different wavelengths and as a function of snow layer thickness and snow type, is expected to be highly relevant in remote sensing applications such as land mapping applications, where differentiation between snow types and snow and vegetated areas are potential applications[15]. Finally, the transmittance of light through snow to an underlying object is expected to be highly relevant in solar energy harvesting modelling and applications in land areas where snowfalls are frequent[27-29], and in biological sciences where the mechanisms behind photosynthesis onset processes during early spring need to be better understood[31].

In future studies we recommend looking further into the validity of the extinction model in predicting characteristic optical material parameters (such as extinction coefficients and transmittance) of snow layers based on reflectance measurements. The extinction model is based on a mathematical model for light penetration through thin, semi-transparent material, and as such, more studies need to be conducted to see if the model holds for snow when snow is treated as a stack of a high number of highly transparent layers. If possible, measurements of snow transmittance should be conducted from 350 to 2500 nm and compared with snow transmittance predicted by the extinction model and based on reflectance data alone.

If the model holds, snow reflectance data should also be captured for layered structures consisting of other types of snow (not just wet and coarse, as in this study), allowing for estimations of extinction coefficient values for all snow types. Snow extinction coefficients should moreover be found for the whole wavelength spectra (350 – 2500 nm) so that transmittance spectra and absorptance spectra of different types of snow can be predicted through simple reflectance measurements.

Downloaded From: https://www.spiedigitallibrary.org/conference-proceedings-of-spie on 18 Oct 2021
Terms of Use: https://www.spiedigitallibrary.org/terms-of-use

A further strengthening of the modelling approach, and in the estimations of the extinction coefficients, can likely be achievable if snow reflectance measurements are conducted on layered snow packs and by varying the spectral signature of the underlying object. This would remove the specificity of the underlying object signature on the estimated extinction coefficients. As an example, we observed this issue when estimating the extinction coefficient at 1100 nm (Fig. 13 and 14) where the difference in underlying object signature and inherent snow signature was minimal, leading to less reliable estimations of the extinction coefficient at this wavelength. We believe the estimations would have been more reliable if another object, with a different reflectance signature, had been used, as the differences in snow signature and object signature would then have been larger.

ACKNOWLEDGMENTS

The works was funded by The Norwegian Defence and Research Establishment (FFI).

The authors have no conflicts of interests.

REFERENCES

1 Warren, S. G. Optical properties of ice and snow. *Phil. Trans. R. Soc. A* **377**, doi:http://dx.doi.org/10.1098/rsta.2018.0161 (2019).
2 Perovich, D. K. Light reflection and transmission by a temperate snow cover. *Journal of Glaciology* **53**, 201-210 (2007).
3 Myrabø, H. K., Lillesæter, O. & Høimyr, T. Portable field spectrometer for reflectance measurements 230 - 2500 nm. *Appl. Opt.* **21**, 2855-2858 (1982).
4 Jersblad, J. & Jacobs, P. Thermal transmission of camouflage nets revisited. *Proc. SPIE* **9997**, 99970S (2016).
5 Jersblad, J. & Larsson, C. Camouflage effectiveness of static nets in SAR images. *Proc. SPIE* **9653**, 965304 (2015).
6 Selj, G. & Heinrich, D. A field-based method for evaluating thermal properties of static and mobile camouflage. *Proc. SPIE* **10794**, 107940B (2018).
7 Racek, F., Jobánek, A., Baláž, T. & Krejčí, J. Selected issues connected with determination of requirements of spectral properties of camouflage patterns. *Proc. SPIE* **10432**, 1043205 (2017).
8 Selj, G. & Heinrich, D. Search by photo methodology for signature properties assessment by human observers. *Proc. SPIE* **9474**, 947411 (2015).
9 Selj, G. & Søderblom, M. *Discriminating between camouflaged targets by their time of detection by a human-based observer assessment method*. Vol. 9653 ESD (SPIE, 2015).
10 Skiles, M. S., Lund, J. & Painter, T. in *IGARSS 2018 - 2018 IEEE INTERNATIONAL GEOSCIENCE AND REMOTE SENSING SYMPOSIUM*. 6287-6290 (IEEE).
11 Varsa, P. M., Baranoski, G. V. G. & Kimmel, B. W. SPLITSnow: A spectral light transport model for snow. *Remote Sens. Environ.* **255**, 112272, doi:https://doi.org/10.1016/j.rse.2020.112272 (2021).
12 Bänninger, D. & Flühler, H. Modelling light scattering at soil surfaces. *IEEE T. Geosci. Remote* **42**, 1462-1471, doi:https://doi.org/10.1109/TGRS.2004.828190 (2004).
13 Mikkelsen, A. & Selj, G. Spectral reflectance and transmission properties of a multi-layered camouflage net: comparison with natural birch leaves and mathematical models. *Proc. SPIE* **11536**, 1153609 (2020).
14 Mikkelsen, A. & Selj, G. Spectral properties of multilayered oak leaves and a camouflage net - experimental measurements and mathematical modelling. *Proc. SPIE* **11865**, 11865-11862 (2021).
15 Negi, H. S., Singh, S. K., Kulkarni, A. V. & Semwal, B. S. Field-based spectral reflectance measurements of seasonal snow cover in the Indian Himalaya. *Int. J. Remote Sens.* **31**, 2393-2417 (2010).
16 Wilhelm, R. H. & Smith, J. B. Transmittance, reflectance, and absorptance of near infrared radiation in textile materials. *Text. Res. J.* **19**, 73-88, doi:10.1177/004051754901900202 (1949).
17 Verhoef, W. Simultaneous retrieval of soil, leaf, canopy, and atmospheric parameters from hyperspectral information in the red edge through model inversion. *Proc. SPIE* **3868**, 380-387 (1999).
18 Melillos, G., Themistocleous, K., Agapiou, A., Michaelides, S. & Hadjimitsis, D. Detecting underground structures in Cyprus using field spectroscopy. *Proc. SPIE* **10773**, 107730A (2018).

Downloaded From: https://www.spiedigitallibrary.org/conference-proceedings-of-spie on 18 Oct 2021
Terms of Use: https://www.spiedigitallibrary.org/terms-of-use

19 Zavvartorbati, A., Dehghani, H. & Rashidi, A. J. Evaluation of camouflage effectiveness using hyperspectral images (Erratum). *J. Appl. Remote Sens.* **12**, 019901 (2018).
20 Jiao, Q., Liu, X., Liu, B., Zhang, X. & Zhang, B. Study on the predicted model of crop leaf water status by the NIR band of ground reflectance and spaceborne hyperspectral images. *Proc. SPIE* **6835**, 68351H (2008).
21 Rosario, D. & Ortiz, A. Spectral-elevation data registration using visible-SWIR spatial correspondence. *Proc. SPIE* **10644**, 106440C (2018).
22 Coppo, P., Chiarantini, L. & Alparone, L. Design and validation of an end-to-end simulator for imaging spectrometers. *Opt. Eng.* **51**, 111721 (2012).
23 Charrois, L. *et al.* On the assimilation of optical reflectances and snow depth observations into a detailed snowpack model. *The Cryosphere* **10**, 1021-1038, doi:doi:10.5194/tc-10-1021-2016 (2016).
24 L., H. C. *et al.* Impact of snow grain shape and black carbon-snow internal mixing on snow optical properties: parametrizations for climate models. *Journal of Climate* **30**, 10019-10036, doi:10.1175/JCLI-D-17-0300.1 (2017).
25 Gatebe, C. K. & King, M. D. Airborne spectral BRDF of various surface types (ocean, vegetation, snow, desert, wetlands, sloud decks, smoke layers) for remote sensing applications. *Remote Sens. Environ.* **179**, 131-138, doi:10.1016/j.rse.2016.03.029 (2016).
26 Franch, B., Vermote, E. F. & Claverie, M. Intercomparison of Landsat albedo retrieval and evaluation against in situ measurements across the US SURFRAD network. *Remote Sens. Environ.* **152**, 627-637, doi:10.1016/j.rse.2014.07.019 (2014).
27 Andenæs, E. *et al.* The influence of snow and ice coverage on the energy generation from photovoltaic solar cells. *Solar Energy* **159**, 318-328 (2018).
28 Andrews, R. W., Pollard, A. & Pearce, J. M. The effects of snowfall on solar photovoltaic performance. *Solar Energy* **92**, 84-97, doi:https://doi.org/10.1016/j.solener.2013.02.014 (2013).
29 Pawluk, R. E., Chen, Y. & She, Y. Photovoltaic electricity generation loss due to snow - A literature review on influence factors, estimation, and mitigation. *Renew Sustain Energy Rev* **107**, 171-182, doi:https://doi.org/10.1016/j.rser.2018.12.031 (2019).
30 Ogaard, M. B. *et al.* Identifying snow in photovoltaic monitoring for improved snow loss modelling and snow detection. *Solar Energy* **223**, 238-247, doi:10.1016/j.solener.2021.05.023 (2021).
31 Robson, T. M. & Aphalo, P. J. Transmission of ultraviolet, visible and near-infrared solar radiation to plants within a seasonal snow pack. *Photochem. Photobiol. Sci.* **18**, 1963-1971, doi:DOI: 10.1039/c9pp00197b (2019).
32 Lillesaeter, O. Spectral reflectance of partly transmitting leaves: Laboratory measurements and mathematical modeling. *Remote Sens. Environ.* **12**, 247-254, doi:https://doi.org/10.1016/0034-4257(82)90057-8 (1982).
33 Palmer, K. F. & Williams, D. Optical properties of water in the near infrared*. *J. Opt. Soc. Am.* **64**, 1107-1110, doi:10.1364/JOSA.64.001107 (1974).
34 Cook, J. M. *et al.* Quantifying bioalbedo: a new physically based model and discussion of empirical methods for characterising biological influence on ice and snow albedo. *The Cryosphere* **11**, 2611-2632, doi:https://doi.org/10.5194/tc-11-2611-2017 (2017).
35 Zhang, J. H., Zhou, Z. M., Wang, P. J., Yao, F. M. & Liming, Y. Spectral Reflectance Characteristics of Different Snow and Snow-Covered Land Surface Objects and Mixed Spectrum Fitting. *Spectroscopy and Spectral Analysis* **31**, 2499-2502, doi:10.3964/j.issn.1000-0593(2011)09-2499-04 (2011).
36 Kokhanovsky, A. A. *et al.* On the reflectance spectroscopy of snow. *The Cryosphere* **12**, 2371-2382, doi:https://doi.org/10.5194/tc-12-2371-2018 (2018).
37 Shekhar, C., Srivastava, S., Negi, H. S., Gore, A. & Snehmani. Effects of linear and non-linear mixing on hyper-spectral signatures of snow in the optical region (350 - 2500 nm). *Geocarto International* **34**, 644-663, doi:ttps://doi.org/10.1080/10106049.2018.1434683 (2019).
38 Shekhar, C., Srivastava, S., Negi, H. S. & Dwivedi, M. Hyper-spectral data based investigations for snow wetness mapping. *Geocarto International* **34**, 664-687, doi:10.1080/10106049.2018.1438528 (2019).
39 Green, O. R., Painter, T., Roberts, D. A. & Dozier, J. Measuring the expressed abundance of the three phases of water with an imaging spectrometer over melting snow. *Water Resources Research* **42**, doi:doi:10.1029/2005WR004509. (2006).
40 Heinrich, D. & Selj, G. Evaluation of camouflage pattern performance of textiles by human observers and CAMAELEON. *Proc. SPIE* **10432**, 1043206 (2017).

Downloaded From: https://www.spiedigitallibrary.org/conference-proceedings-of-spie on 18 Oct 2021
Terms of Use: https://www.spiedigitallibrary.org/terms-of-use